Attribute mapping of variable-thickness incised valley-fill systems

Fangyu Li[1], Jie Qi[1], and Kurt Marfurt[1]

Abstract

Whether we realize it or not, seismic amplitude is the composite expression of multiple frequency components. Spectral components tuned to a given thickness often exhibit a high signal-to-noise ratio and thus provide the highest lateral resolution, giving clear images of channels and other stratigraphic features that otherwise might be buried in broadband data. For the same reason, coherence and other edge-sensitive attributes provide correspondingly sharper images when computed from spectral-magnitude or voice components. Multiple stages of incisement are preserved in a survey acquired over the Red Fork Formation of the Anadarko Basin, Oklahoma. Color-blended images of 20-, 35-, and 50-Hz spectral components and corresponding coherence images are used to map the valley fill at different stages.

Introduction

The broadband seismic response of a given geologic feature is composed of its response of its constituent spectral bands. Through constructive and destructive interference, the resulting vertical and horizon slices often represent the response of the strongest or dominant frequency corresponding to structure and stratigraphy of given-time tuning thickness in the analysis window. Spectral-decomposition methods map 1D seismic amplitude into 2D time and frequency spectral magnitude and phase components (Partyka et al., 1999). Analysis of a suite of spectral components within a zone of interest often can provide a more precise perspective of a given geologic structure.

In addition, spectral attributes of narrower-band components can be used to identify anomalous geologic features that otherwise are buried in the broadband seismic response. Not all spectral components contain signal, and others might be overly contaminated by noise. For example, Fahmy et al. (2005) recognize that a deep reservoir tuned at 11 Hz was masked by strong, higher-frequency multiples. By simply removing the high-frequency "signal," they obtained a clear image of the reservoir and performed an accurate AVO analysis.

Estimates of seismic coherence (Bahorich and Farmer, 1995; Marfurt et al., 1998; Gerstzenkorn and Marfurt, 1999), which can highlight changes in seismic waveform or amplitude across a discontinuity, provide a quantitative measure of geologic discontinuity. However, such boundaries and edges computed from broadband seismic data do not give a measure of the vertical scale of the discontinuity. Li and Lu (2014) show that coherence computed from different spectral components can be combined to provide a qualitative measure of the scale of geologic discontinuities such as faults, channels, caves, and collapse features.

In this article, we apply the same workflow that Li and Lu (2014) propose to map variations of thickness and edges to map the different stage fills of incised-valley systems. We use a red-green-blue (RGB) color-blending technique to integrate attributes computed at different spectral components. The data volume is part of a megamerge survey from CGGVeritas over the Anadarko Basin, Oklahoma, and incorporates a survey which was one of the first applications of spectral decomposition interpreted by Peyton et al. (1998) using 36-Hz spectral component and full-band coherence. Although our analysis of the megamerge survey corresponds well with the original incised-valley interpretation, the improved data quality resulting from surface-consistent deconvolution and statics and the larger migration aperture results in much sharper channel images.

Data description

The study area is in the eastern part of the Anadarko Basin, Oklahoma (Figure 1). Pennsylvanian rocks throughout most of the Anadarko Basin are dominated by shallow-shelf marine clastics. The target is the Red Fork Sand of the middle Pennsylvanian. It lies at an approximate depth of 2680 m (~ 8800 ft) and is composed of clastic facies deposited in a deep-marine (shale/silt) to shallow-water fluvial-dominated environment. The Red Fork Sandstone is sandwiched between limestone layers, with the Pink Limestone on top and the Inola Limestone on the bottom. The Oswego Limestone that lies above the Pink Limestone and the Novi Limestone that lies below the Inola Limestone

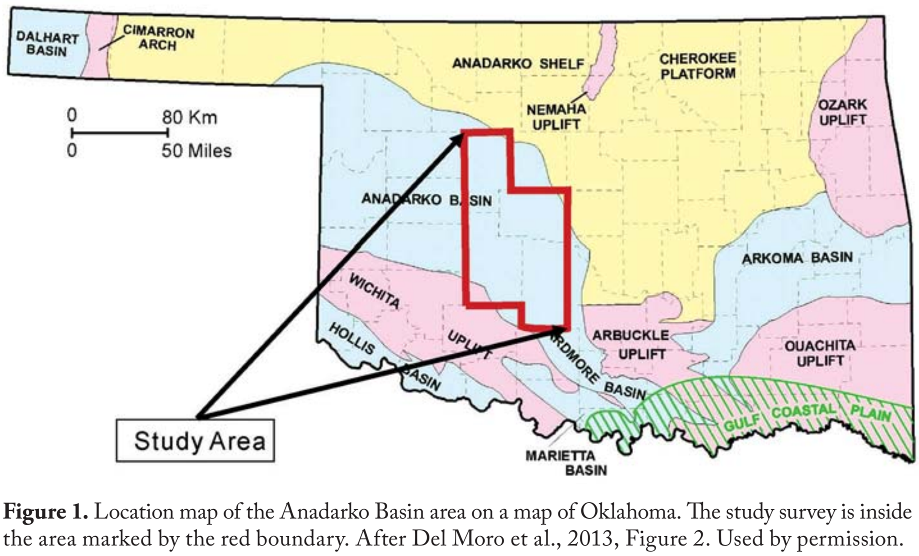

Figure 1. Location map of the Anadarko Basin area on a map of Oklahoma. The study survey is inside the area marked by the red boundary. After Del Moro et al., 2013, Figure 2. Used by permission.

[1]University of Oklahoma.

http://dx.doi.org/10.1190/tle34010048.1.

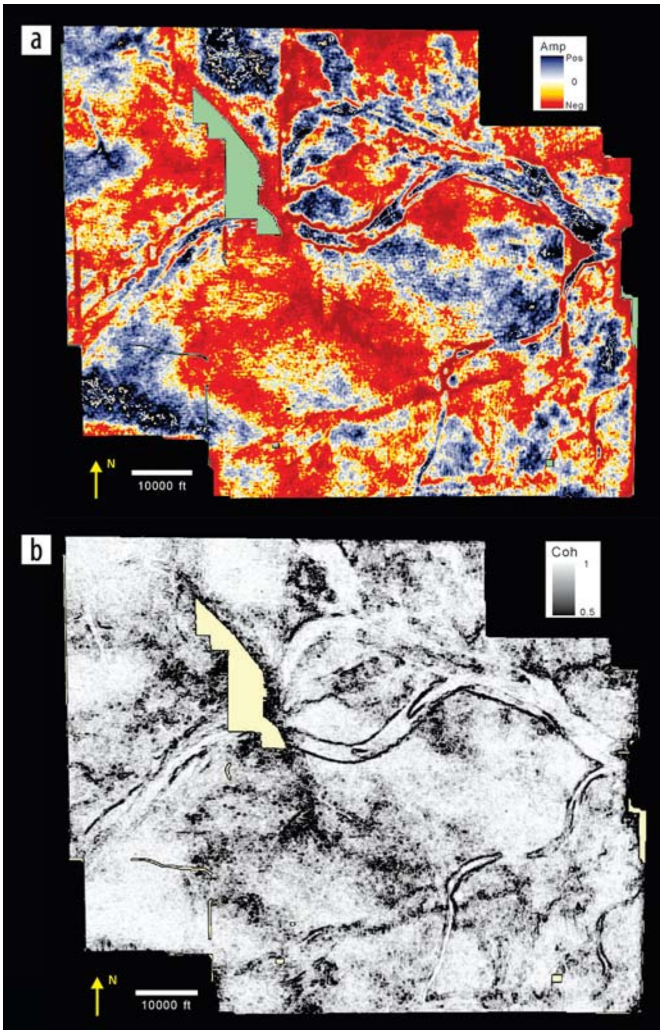

Figure 2. Stratal slices through (a) seismic amplitude and (b) coherence volumes through the Red Fork Formation for the megamerge survey. Note that the edges of the incised valley are shown on the coherence slice. Data courtesy of CGGVeritas. Used by permission.

are prominent reflectors that can be mapped readily on seismic-amplitude data, providing an approximation to a fixed geologic time. The Upper Red Fork incised-valley system consists of multiple stages of incision and fill, resulting in a stratigraphically complex internal architecture.

The survey of interest was shot at various times beginning in the mid-1990s. CGGVeritas acquired licenses for the surveys, shot infill data in 2009 where necessary, and carefully reprocessed them, resulting in a megamerge survey. In addition to more modern statics and deconvolution algorithms, the most significant advantage of the megamerge survey is the inclusion of a wider migration aperture, whereby previously independently processed surveys are allowed to image steeply dipping faults and stratigraphic edges of their neighbors (Del Moro et al., 2013).

The incised valleys are characterized by discontinuous reflections of varying amplitude which are difficult to interpret laterally (Peyton et al., 1998). It is difficult to interpret the Red Fork incised valley using traditional interpretation techniques (autopicking horizons, amplitude mapping, and so forth). Individual stages of fill are almost impossible to identify.

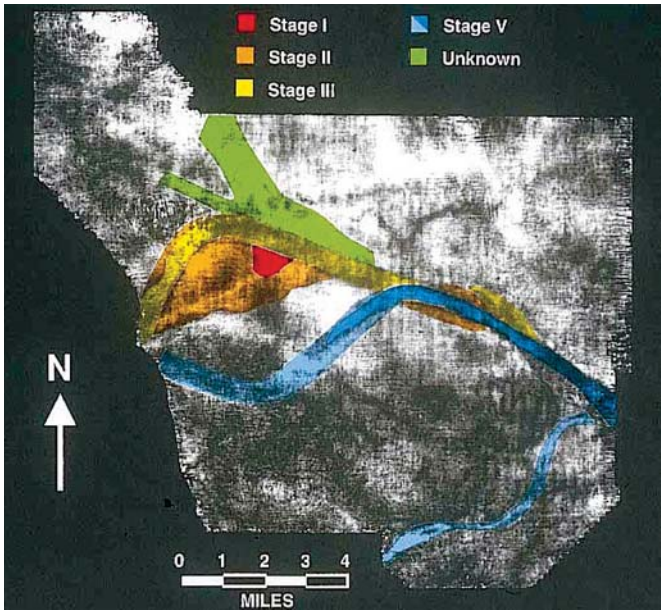

Figure 3. Peyton et al.'s (1998) original slice with interpretation through the 36-Hz spectral magnitude computed from the original 1995 seismic data volume. This same data volume formed part of the megamerge shown in Figure 2.

Attribute expression on valley fill

Figure 2 displays Red Fork stratal slices through the seismic amplitude and coherence volumes. Vertical slices through the seismic amplitude provide an indication of erosion but do not allow one to identify the various stages of valley fill. The coherence attribute in Figure 2b was computed volumetrically from the broadband seismic data. As expected, it images the boundaries of the valley and some internal incisements, but the overall internal detail is diffuse. The main reason for this lack of detail is that coherence was computed from broadband seismic amplitude, and thus it measures a mix of valley-fill stages in the same image. In contrast, lateral changes in sedimentary layers and channel incisement of a given thickness are often imaged better near their tuning thickness.

The Red Fork incised valley can be mapped using spectral components between about 20 and 50 Hz. Peyton et al. (1998) chose a 36-Hz amplitude slice as the best images of the valley throughout the survey area, resulting in the image shown in Figure 3. Their coherence example represents channel features illuminated by the dominant-frequency components.

The cartoon by Laughlin et al. (2002) in Figure 4 shows how thicker and thinner stratigraphic features will be tuned in at correspondingly lower- or higher-frequency components. In practice, the interpreter animates through a suite of spectral components and stops the animation when a particular feature of interest is delineated well.

The same strategy should be adopted in valley-fill analysis. Figure 5 shows the dominant-frequency map of the Red Fork Formation. Different types of geologic structures and different stages of valley fill, each with its own tuning thickness, give rise to anomalies at different dominant frequencies. Spectral magnitude and coherence corresponding to those tuned frequencies provide clearer images.

Although spectral decomposition reveals more details, it generates a series of maps or volumes at different frequencies, which are analyzed one by one or through animation. Blending of RGB images has long been used to express multiple spectral components in a single image (Balch, 1971). Leppard et al. (2010) give an exposition on the value of RGB in rendering multiple spectral images of channels.

We use RGB color-blending technique in Figure 6 to display the 20-, 35-, and 50-Hz spectral components. As shown in the RGB color map, if the energies in all three color channels are at or above the threshold amplitude, the blended color is white, whereas if the energy of one channel is stronger than the other two, its color would dominate.

The color changes provide a good deal of new information. The 20-Hz component is plotted against red and better delineates Stages II, III, and V. The 35-Hz component is plotted against green and delineates medium-thickness Stage V channels. The 50-Hz component is plotted against blue and delineates thinner Stage V channels and part of Stage III.

Compared with the interpretation shown in Figure 3, which is part of our survey, we can observe that the stages interpreted in different colors by Peyton et al. (1998) also display in different colors. Although Stage I is not clearly separated from Stage II or III and the separation cannot be achieved either on single-frequency slice interpretation such as in Peyton et al. (1998), other stages and some geologic structures in other parts of the survey are displayed with different temporal tuning thickness. Other good methods can analyze variance in tuning thickness, but none is as easy to create or is used as routinely.

To use spectral decomposition, it is critical to decide, based on relative amplitudes, which spectral component is a meaningful indicator for a given structure presence. Using animation, we selected 20, 35, and 50 Hz to compare to Peyton et al.'s (1998) 36-Hz component image in Figure 3.

Next, in Figure 7, we compute coherence from each of these spectral components, providing a measure of the edges sensitive to the relative thicknesses of the different stages of valley fill. As to the principles of RGB color blending mentioned above, because the coherence attribute defines the value of coherent reflection equals 1 whereas discontinuity displays a value lower than 1, the areas of white (light gray) are where all three frequency bands are coherent.

On the other hand, the black (dark gray) lines are the channel boundaries which appear on all the selected frequency components. It is interesting that because of the low value of channel edges on the coherence map, the boundaries of relatively thick channels showing on lower-frequency components painted red would appear as cyan after blending, which is the opposite of red on the RGB chart, but edges of thinner channels in part of Stage III and Stage V appear red or yellow.

Because the channel edges can be characterized by other frequency bands, the channel edges shown in Figure 7 are not as numerous as those in Figure 2b. In addition, for most of the area of the image without channel boundaries, the color delegates the change of coherent energy. For example, the large pink (the opposite of green) area implies lower coherent energy in the middle-frequency component.

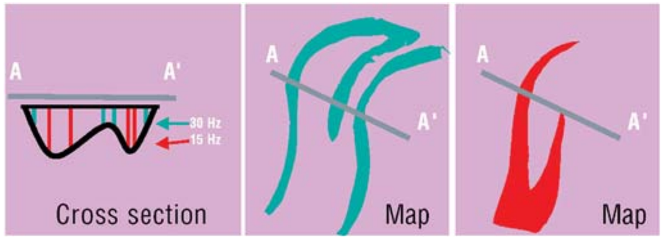

Figure 4. A cartoon of thin-bed tuning. (a) In thin reservoirs with varying thickness, (b) seismic data with higher dominant frequency would highlight the thinner parts of the reservoir on amplitude maps, whereas (c) seismic with lower dominant frequency would highlight the thicker parts on an amplitude map. After Laughlin et al., 2002, Figure 2. Used by permission.

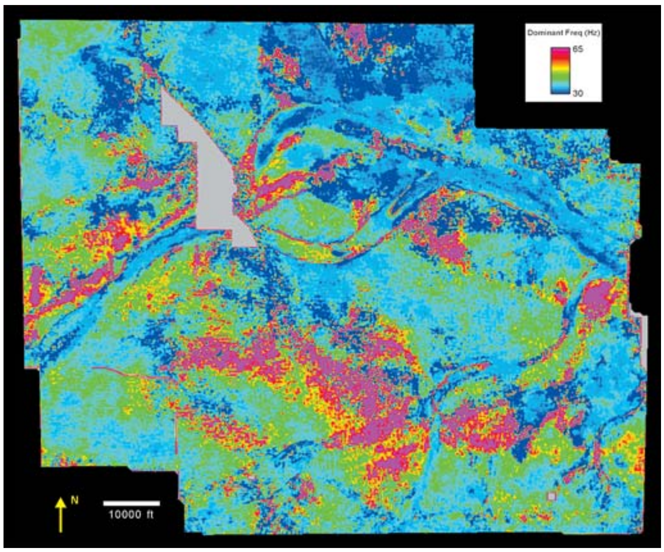

Figure 5. Dominant (or peak) spectral-frequency image of the Red Fork horizon, which shows that the target horizon has different tuning thicknesses. The magnitude of the spectral component is plotted against a gray scale, thereby modulating the image.

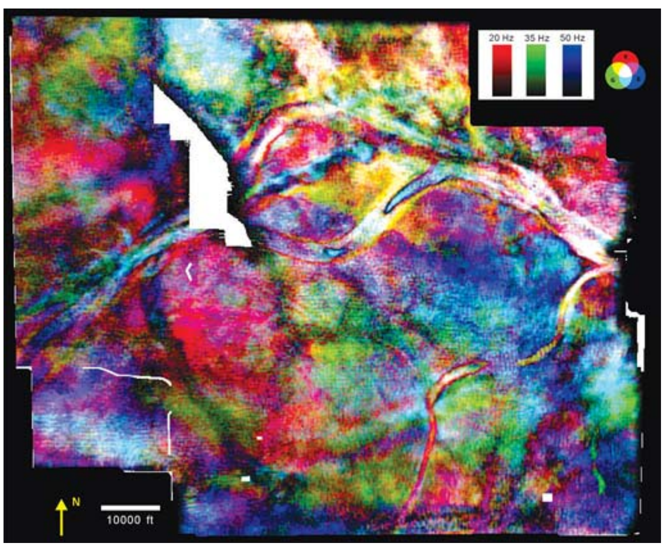

Figure 6. RGB-blended spectral-magnitude components at 20 Hz (in red), 35 Hz (in green), and 50 Hz (in blue).

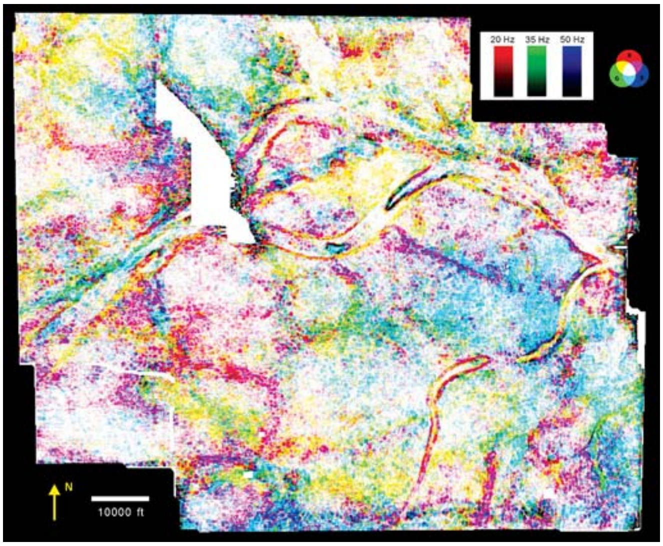

Figure 7. RGB-blended image of coherence corresponding to Figure 6 computed from spectral components at 20 Hz (in red), 35 Hz (in green), and 50 Hz (in blue).

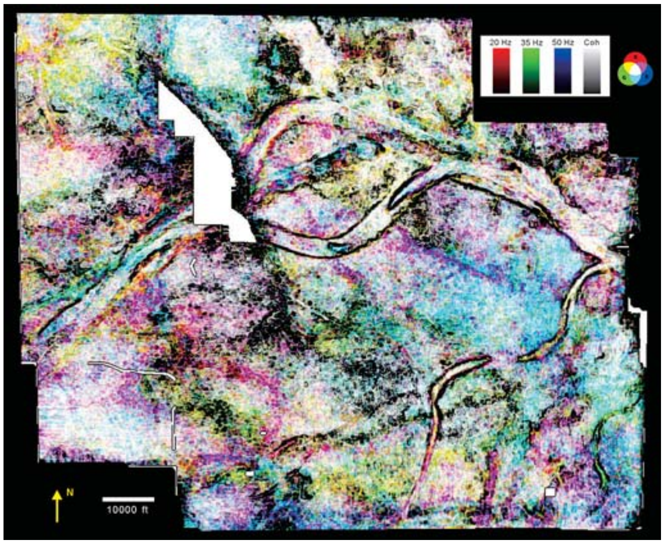

Figure 8. The same image shown in Figure 7 but corendered with that of Figure 2b. Edges that are not overprinted in black were delineated by coherence computed from the corresponding spectral components but not by the broadband coherence computation.

Figure 8 is an overlay of the RGB-blending map shown in Figure 7 and the broadband coherence image shown in Figure 2b. Comparing Figure 8 with Figure 7, we can clearly observe the advantage brought by spectral component coherences. Through the colorful-attribute integration image, we are aware of thickness.

Thus, by more fully using the spectral components (Figure 6) with their corresponding coherence map (Figure 8), stage identification and valley-fill boundary delineation can be interpreted more easily and fully.

Conclusions

Spectral decomposition enhances the response of thin-bed reflections about the tuning frequency. The interpretation of incised valley fill can be difficult on conventional amplitude volumes. By revisiting one of the first data sets analyzed using spectral decomposition and using more modern RGB display techniques, we show the improvements in the spectral-decomposition response of a recent megamerge volume and the additional information obtained by computing coherence of the spectral-component volumes. TLE

Acknowledgments

We thank CGGVeritas for permission to use its megamerge seismic survey. Funding for the research was provided by the industry sponsors of the Attribute-Assisted Seismic Processing and Interpretation Consortium (AASPI) at the ConocoPhillips School of Geology and Geophysics, University of Oklahoma.

Corresponding author: fangyu.li@ou.edu

References

Bahorich, M. S., and S. L. Farmer, 1995, 3-D seismic discontinuity for faults and stratigraphic features: The coherence cube: The Leading Edge, **14**, no. 10, 1053–1058, http://dx.doi.org/10.1190/1.1437077.

Balch, A. H., 1971, Color sonograms: A new dimension in seismic data interpretation: Geophysics, **36**, no. 6, 1074–1098, http://dx.doi.org/10.1190/1.1440233.

Del Moro, Y., A. Fernandez-Abad, and K. J. Marfurt, 2013, Why should we pay for a merged survey that contains data we already have? An OK Redfork example: Shale Shaker, **63**, no. 5, 340–363.

Fahmy, W. A., G. Matteucci, D. Butters, J. Zhang, and J. Castagna, 2005, Successful application of spectral decomposition technology toward drilling of a key offshore development well: 75th Annual International Meeting, SEG, Expanded Abstracts, 262–264, http://dx.doi.org/10.1190/1.2144316.

Gersztenkorn, A., and K. J. Marfurt, 1999, Eigenstructure-based coherence computations as an aid to 3-D structural and stratigraphic mapping: Geophysics, **64**, no. 5, 1468–1479, http://dx.doi.org/10.1190/1.1444651.

Laughlin, K., P. Garossino, and G. Partyka, 2002, Spectral decomposition applied to 3D: AAPG Explorer, **23**, no. 5, 28–31.

Leppard, C., A. Eckersley, and S. Purves, 2010, Quantifying the temporal and spatial extent of depositional and structural elements in 3D seismic data using spectral decomposition and multi attribute RGB blending, *in* L. J. Wood, T. T. Simo, and N. C. Rosen, eds., Seismic imaging of depositional and geomorphic systems: 30th Annual GCSSEPM Foundation Bob F. Perkins Research Conference, 1–10.

Li, F. Y., and W. K. Lu, 2014, Coherence attribute at different spectral scales: Interpretation, **2**, no. 1, SA99–SA106, http://dx.doi.org/10.1190/INT-2013-0089.1.

Marfurt, K. J., R. L. Kirlin, S. L. Farmer, and M. S. Bahorich, 1998, 3-D seismic attributes using a semblance-based coherency algorithm: Geophysics, **63**, no. 4, 1150–1165, http://dx.doi.org/10.1190/1.1444415.

Partyka, G. A., J. Gridley, and J. Lopez, 1999, Interpretational applications of spectral decomposition in reservoir characterization: The Leading Edge, **18**, no. 3, 353–360, http://dx.doi.org/10.1190/1.1438295.

Peyton, L., R. Bottjer, and G. Partyka, 1998, Interpretation of incised valleys using new-3D seismic techniques: A case history using spectral decomposition and coherency: The Leading Edge, **17**, no. 9, 1294–1298, http://dx.doi.org/10.1190/1.1438127.